SSRG International Journal of Electrical and Electronics Engineering
ISSN: 2348-8379/ https://doi.org/10.14445/23488379/IJEEE-V11I4P112

Volume 11 Issue 4, 109-117, April 2024

Original Article

Analysis of Processes of Image Formation of Bio-Objects Based on Gas Discharge Visualization

Natalia Kosulina[1], Maksym Sorokin[2], Yuri Handola[3], Stanislav Kosulin[4], Kostiantyn Korshunov[5], Mariia Chorna[6], Vitaly Sukhin[7]

[1,2,3,5,6,7]*Department of Electromechanics, Robotics, Biomedical and Electrical Engineering, State Biotechnological University, Ukraine.*
[4]*Department of Oncosurgery Radiation Therapy and Palliative Care, Kharkiv National Medical University, Kharkiv, Ukraine.*

[1]*Corresponding Author : kosnatgen@ukr.net*

Received: 08 February 2024 Revised: 09 March 2024 Accepted: 07 April 2024 Published: 30 April 2024

Abstract *- The application of an information polarized electromagnetic field in resource-saving, low-energy electromagnetic crop production technologies with the introduction of automated systems of gas-discharge visualization of bio-objects into the technological cycle of pre-sowing seed treatment is shown. The process of forming a gas-discharge image of a bio-object located in the recess of a flat electrode and on a rectangular protrusion of one flat electrode is considered. Based on the application of the complex potential method, which is based on conformal maps of a simple region on one complex plane to a real Region obtained on the second complex plane, expressions were obtained on the basis of which calculations of the distribution of electric field strength for various variants were performed. The distribution of the electric field strength is determined between the plates of the gas-discharge cell, when a<b, a<l, V = 15 kV, a = 6 mm, connecting the voltage source in the center above the protrusion, that is, without displacement; between the plates of the gas-discharge cell, when a a< b, a< l, V = 20 kV, a = 6 mm, the offset from the center of the recess of the voltage source connection point is 10 mm. and above the protrusion of the cell electrode, when a = b = 6 mm; V = 20 kV when connecting a high-voltage voltage source in the center above the protrusion, i.e. without displacement; above the protrusion on the cell electrode when a = b = 6 mm, V = 15 kV when connecting a high-voltage voltage source in the center above the protrusion, that is, without displacement; above the protrusion on the cell electrode when a = b = 6 mm, V = 20 kV when connecting a voltage source with a shift from the center by 10 mm. Based on the graphical dependences of the electric field strength, it is justified to obtain a high-quality gas-discharge visualization of a biological object. It is shown that the studied biological object, for example, a small seed, should be placed on the surface of the protrusion of the cell electrode with a distance between the protrusion and the second electrode of the cell of a gas-discharge visualization device of 1 mm, and a high-voltage voltage source of 15...20 kV should be connected in the center of the protrusion without displacement in order to ensure the non-invasiveness of gas-discharge visualization, an assessment of the energy of thermal processes and their impact on the bio-object was carried out.*

Keywords *- Biological object, Gas-Discharge Visualization, Electric field, Tension, High-voltage.*

1. Introduction

Currently, in agricultural production, numerous attempts are being made to use electromagnetic energy to affect the seeds of agricultural crops. So, for example, pre-sowing treatment of cereal seeds with electromagnetic radiation (EMR) with thermal power levels increases their similarity by 2-3%, the yield is 10-16%, while the quality indicators can be compared with the control material [1-3]. Thermal methods of impact on biological objects are not always applicable in agriculture. They can be dangerous for human health and significantly increase the price of products; in addition, there is mostly no repeatability of obtaining a positive effect from their use. Of particular interest and significance is the application of the informational polarized Electromagnetic Field (EMF) to biological objects to increase the quality and quantity of the harvest, disinfect seeds, treat animals, and combat agricultural pests.

The use of information EMF in agricultural production is associated with the lowest energy consumption with maximum impact on the information processes of the vital activity of biological objects, which do not depend on the magnitude of the radiation energy affecting it but on the corresponding frequency and modulation-time parameters EMF [4-8]. The relevance of these studies is confirmed by discoveries, inventions, including in agricultural

bioelectromagnetology, and foreign works related to the purposeful use of EMF information radiation not only on animals and plants, but also on humans. However, the maximum (desired) changes in the properties of this biological object (taking into account the state of the external environment) can be obtained only with an optimal combination of biotropic EMF parameters. Determining the biotropic parameters of EMF using agrotechnical methods is time-consuming and, in addition, their determination requires considerable time [9-16].

With the proper selection of the parameters of the EMF affecting the biological object, it is possible to change the course of information processes in the biological object and mobilize its forces to obtain the intended biological effect. Accordingly, there is a need to conduct theoretical studies to determine the range of changes in biotropic EMF parameters and optimize these parameters with the help of data obtained from automated devices for Gas Discharge Visualization (GDV) of biological objects.

Insufficient theoretical research and incomplete automated devices for determining the biotropic parameters of EMF and forming the image of bioobjects based on GDV limit the possibility of purposeful application of EMF, complicate the analysis of phenomena and leave a problematic question regarding the creation of resource-saving electromagnetic technologies in agricultural production [16-19].

The creation of resource-saving informational electromagnetic technologies in crop production based on the application of informational polarized EMF is possible only with the introduction into the technological cycle of pre-sowing treatment of seeds of automated systems GDV of bioobjects.

Taking into account, the phenomenon of gas discharge visualization is associated with the presence of significant gradients in the distribution of the electric field between the surface of the substance under investigation, which is located on one of the electrodes of the GDV cell of the device, and the second electrode. The presence of these gradients in the case when the electric field strength is quite high (tens of kV/cm) will lead to different intensities of avalanche discharges, which, in turn, will depend on the location of the biological object in the cell of the GDV device, the size of the biological object and the distance between the covers of the cell of the GDV device, as well as from the point of connection of the high-voltage voltage source.

Taking into account the above, the work aims to analyze the processes of image formation of bioobjects based on gas discharge imaging to determine the biotropic parameters of EMF, which cause an increase in the productivity of bioobjects of crop production when they interact with informational polarized EMF of the microwave range.

2. Materials and Methods

As is known, any electrostatic field is potential [1, 2]. In the case when a flat electrostatic field $\vec{E} = \{E_x, E_y\}$ is considered, the condition [1, 2] is fulfilled:

$$\left(\overrightarrow{rot\,E}\right)_n = \frac{\partial E_y}{\partial x} - \frac{\partial E_x}{\partial y} = 0, \quad (1)$$

or

$$-\frac{\partial E_y}{\partial x} = -\frac{\partial E_x}{\partial y}. \quad (2)$$

Noting: $P = -E_x$; $Q = -E_y$ and taking into account that equality $\frac{\partial Q}{\partial x} = \frac{\partial P}{\partial y}$ is a necessary and sufficient condition that the expression:

$$dv = Qdx + Pdy = -E_x dx - E_y dy = \\ = \frac{\partial v}{\partial x}dx + \frac{\partial v}{\partial y}dy \quad (3)$$

Equation 3 will be the complete differential of the function, we can conclude that the function itself can be restored using the expressions [20, 21]:

$$v(x,y) = -\int_{(x_0,y_0)}^{(x,y)} E_x dx + E_y dy + C_1. \quad (4)$$

In expression (4), we take the curvilinear integral along an arbitrary contour L that connects a fixed point (x_0, y_0) with a variable point (x, y) Moreover, it has no special points. The constant is determined from the given initial conditions.

Using expression (3), the electromagnetic field vector can be represented in the form [20, 21]:

$$\vec{E} = E_x\vec{\imath} + E_y\vec{\jmath} = -\frac{\partial v}{\partial x}\vec{\imath} - \frac{\partial v}{\partial y}\vec{\jmath} = -\,grad\,v, \quad (5)$$

Where $\vec{\imath}$ and $\vec{\jmath}$ are orthogonal directed along the axes OX and OY.

The function $v = v(x, y)$ is called potential, and its level lines are called equipotential lines.

Let us now take into account that the space between the electrodes containing the material under study does not contain sources of charges. In this case, as is known [20, 21], the electrostatic field $\vec{E}$ is solenoidal:

$$\overrightarrow{div\,E} = \frac{\partial E_x}{\partial x} + \frac{\partial E_y}{\partial y} = 0, \quad (6)$$

or

$$\frac{\partial E_x}{\partial x} = -\frac{\partial E_y}{\partial y}. \quad (7)$$

By analogy with the above, condition (7) is also a necessary and sufficient condition for the expression:

$$du = -E_y dx + E_x dy = \frac{\partial u}{\partial x} dx + \frac{\partial u}{\partial y} dy \qquad (8)$$

Equation 8 will be the complete differential of the function $u = u(x, y)$. At the same time, this function is restored by its complete differential using a similar expression (4) of the curvilinear integral:

$$u(x, y) = \int_{(x_0, y_0)}^{(x,y)} -E_y dx + E_x dy + C_2. \qquad (9)$$

Thus, two scalar functions correspond to a flat electrostatic field in the absence of charges: the potential function $v(x, y)$ and the function $u(x, y)$.

Let us now consider these functions from a slightly different angle. It follows from expression (5) that:

$$E_x = -\frac{\partial v}{\partial x}, E_y = -\frac{\partial v}{\partial y}, \qquad (10)$$

and from expression (8):

$$E_x = \frac{\partial u}{\partial y}, E_y = -\frac{\partial u}{\partial x}. \qquad (11)$$

So,

$$\frac{\partial u}{\partial x} = \frac{\partial v}{\partial y}, \frac{\partial u}{\partial y} = -\frac{\partial v}{\partial x}. \qquad (12)$$

But these conditions are nothing but Cauchy-Riemann conditions for the real $u(x, y)$ and imaginary $v(x, y)$ part of the analytic function w of a complex argument z [20, 21]:

$$w = f(z) = u(x, y) + iv(x, y), \qquad (13)$$

Where $z = x + iy$; i – imaginary unit.

It follows from the obtained result that the function level lines $u(x, y)$ and $v(x, y)$ are orthogonal [21]. But the electric field vector $\vec{E}$ is normal to the lines of the level of the potential function $v(x, y)$, respectively, it will be tangent to the lines of the level of the function $u(x, y)$, which, accordingly, is called the force function of the field. In this case, the function $w = f(z)$ is called the complex potential of the electrostatic field under consideration.

It should be noted that since the derivative of the complex potential is uniquely determined by expressions (12), using the rule for its calculation, we obtain:

$$f'(z) = \frac{\partial u}{\partial x} + i\frac{\partial v}{\partial x} = \frac{\partial v}{\partial y} + i\frac{\partial v}{\partial x} = \\ = -E_y - iE_x = -i(E_x - iE_y). \qquad (14)$$

It follows that:

$$E_x - i E_y = i f'(z). \qquad (15)$$

Since, from a geometric point of view, a complex number is nothing but a vector on a plane, we obtain from the expression (15):

$$\vec{E} = E_x \vec{i} + E_y \vec{j} = E_x + i E_y = -i \overline{f'(z)}, \qquad (16)$$

Where a dash above the derivative indicates that a complex conjugate value is taken.

It also follows from expression (16) that the value of the tension vector is:

$$|\vec{E}| = \left|-i\overline{f'(z)}\right| = \sqrt{\left(\frac{\partial v}{\partial x}\right)^2 + \left(\frac{\partial v}{\partial y}\right)^2}. \qquad (17)$$

It follows from the above that the complex potential maps the flat of the field z onto the flat w, conformal at all points of the field region, where its intensity differs from zero. But since the level lines $u(x, y) = const$ and $v(x, y) = const$ are mutually perpendicular; they will be parallel to the real OU and imaginary OV coordinate axes.

Accordingly, knowing the complex potential of the field, it is possible to find its equipotential and force lines and, with them, the entire picture of the field.

3. Results

Let us consider the case when the bioobject is placed in a recess on the flat electrode of the cell of the GDV device, while the width of this recess a is much smaller than its depth b and the distance between the electrodes l (Figure 1).

$$z = \frac{a}{\pi}\left(\sqrt{w^2 - 1} + arcsin\frac{1}{w}\right). \qquad (18)$$

At the same time, the transformation itself looks as follows (Figure 1):

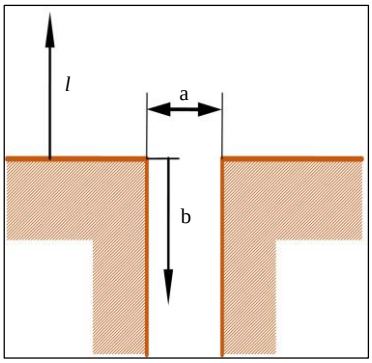

Fig. 1 Case of indentation with parameters $b > a$, $l > a$ on the electrode

The conformal transformation, which displays the upper half-plane on the complex plane w corresponding to the complex potential $w = u + iv$, on the half-plane with a cut in the complex plane z, which coincides with the electrode under consideration, has the form (Figure 2):

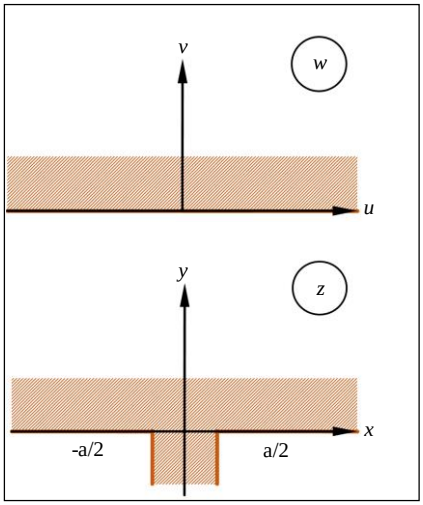

Fig. 2 Conformal transformation of a half-plane on the complex plane w into a half-plane with a cut on the complex plane z

In the same way as above, to solve the given problem, we will find x, y, E_x та E_y. It follows from expression (18) that:

$$x = Re\, z = \frac{a}{\pi}\left(\sqrt[4]{\left(\frac{u^2-v^2}{u^2+v^2}-1\right)^2} + \frac{(2uv)}{u^2+v^2}cos\,\frac{\phi}{2} + \right.$$
$$\left. + arcsin\,\frac{2u^2/u^2+v^2}{N+P}\right); \quad (19)$$

$$y = Im\, z = \frac{a}{\pi}\left(\sqrt[4]{\left(\frac{u^2-v^2}{u^2+v^2}-1\right)^2} + \frac{(2uv)}{u^2+v^2}sin\,\frac{\phi}{2} - \right.$$
$$\left. - arch\,\frac{N+P}{2}\right); \quad (20)$$

$$N = \sqrt{\left(1+\frac{u^2}{u^2+v^2}\right)^2 + \left(\frac{v^2}{u^2+v^2}\right)^2}; \quad (21)$$

$$P = \sqrt{\left(1-\frac{u^2}{u^2+v^2}\right)^2 + \left(\frac{v^2}{u^2+v^2}\right)^2}; \quad (22)$$

$$\phi = arctg\,\frac{2uv}{u^2-v^2}. \quad (23)$$

Using data:

$$E_x = Re\left(-i\,\overline{\frac{dw}{dz}}\right) = Re\left(-i\,\overline{\frac{1}{\frac{dz}{dw}}}\right) =$$
$$= Re\left(-i\,\overline{\frac{1}{\frac{\partial x}{\partial u}+i\frac{\partial y}{\partial u}}}\right) =$$
$$= Re\,\frac{\frac{\partial y}{\partial u}-i\frac{\partial x}{\partial u}}{\left(\frac{\partial x}{\partial u}\right)^2+\left(\frac{\partial y}{\partial u}\right)^2} = \frac{\frac{\partial y}{\partial u}}{\left(\frac{\partial x}{\partial u}\right)^2+\left(\frac{\partial y}{\partial u}\right)^2},$$

$$E_y = Im\left(-i\,\overline{\frac{dw}{dz}}\right) = Im\,\frac{\frac{\partial y}{\partial u}-i\frac{\partial x}{\partial u}}{\left(\frac{\partial x}{\partial u}\right)^2+\left(\frac{\partial y}{\partial u}\right)^2} = \frac{-\frac{\partial x}{\partial u}}{\left(\frac{\partial x}{\partial u}\right)^2+\left(\frac{\partial y}{\partial u}\right)^2}.$$

We define:

$$E_x = \frac{\pi}{a}\,\frac{u\,sin\frac{\phi}{\pi}-v\,cos\frac{\phi}{\pi}}{\sqrt[4]{\left(\frac{u^2-v^2}{u^2+v^2}-1\right)+\frac{(2uv)^2}{u^2+v^2}}}; \quad (24)$$

$$E_y = \frac{\pi}{a}\,\frac{u\,cos\frac{\phi}{\pi}-v\,sin\frac{\phi}{\pi}}{\sqrt[4]{\left(\frac{u^2-v^2}{u^2+v^2}-1\right)+\frac{(2uv)^2}{u^2+v^2}}}. \quad (25)$$

The simulation of the distribution of the electric field strength over the surface of the depression of the tray with the bioobject, when the distance to the second electrode is much greater than the width of this tray, allowed us to obtain the expression (19-25).

Numerical calculations of the dependence of the electric field strength between the electrodes of the cell, when the applied potential between them is equal to 15 kV and 20 kV (Figures 3 and 4) were performed.

The graphs in Figures 3 and 4 are plotted for the width of the recess a = 6 mm. The change of x on the horizontal axis corresponds to the size of the electrode of the GDV cell of the device, which has the shape of a circle. The voltage source is connected in the center of the cell circle (Figure 3). Curve 1 on the graph corresponds to a distance between electrodes of 20 mm, curve 2 – 30 mm, curve 3 – 60 mm.

It follows from the graph (Figure 3) that the maximum electric field intensity is located above the middle of the recess and is 7 kV/cm ($a/l = 0{,}3$) at a voltage source of 15 kV.

The obtained dependences (Figure 3) for the electric field intensity between the covers of the device's GDV cell show that, in this case, there will be no GDV of the biological object.

It follows from the graphs (Figure 4) that as the distance between the electrodes of the cell increases, the intensity of the electric field between them decreases, and the maximum intensity shifts to the point of connection of the voltage source.

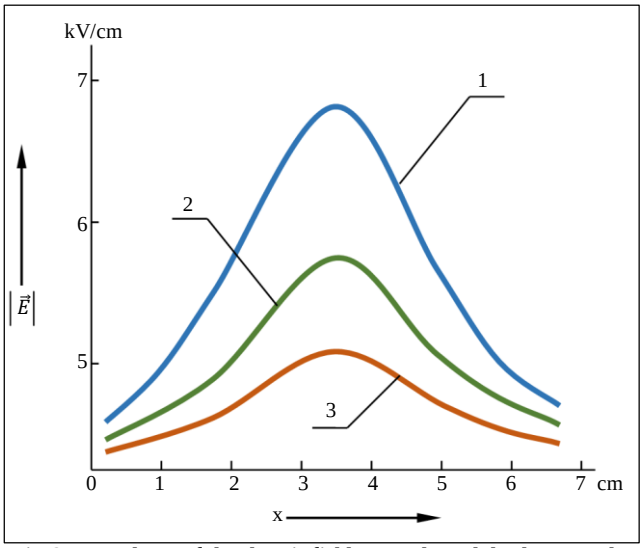

Fig. 3 Dependence of the electric field strength modulus between the plates of the cell when $a < b$, $a < l$, V = 15 kV, a = 6 mm. Connecting the voltage source in the center above the protrusion, i.e. without offset: 1) $a/l = 0,3$; 2) $a/l = 0,2$; 3) $a/l = 0,1$

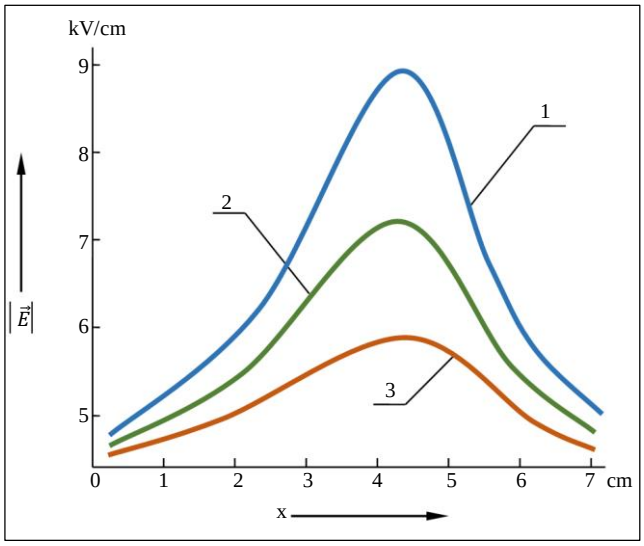

Fig. 4 Dependence of the voltage of the electric field between the plates of the cell, when $a < b$, $a < l$, V = 20 kV, a = 6 mm. The shift from the center of the depression of the voltage source connection point is 10 mm: 1) $a/l = 0,3$; 2) $a/l = 0,2$; 3) $a/l = 0,1$

From the obtained dependencies (Figure 4), it follows that increasing the voltage of the power source to 20 kV will not lead to the appearance of electronic and ion emissions.

It follows from the calculations that it is possible to find the optimal value of the applied potential after experimental refinement of the obtained theoretical results.

However, there may be cases when it is expedient and convenient to place a biological object on the protrusion of one of the cell's electrodes. For simplicity, we will consider the profile of this protrusion to be rectangular (Figure 5).

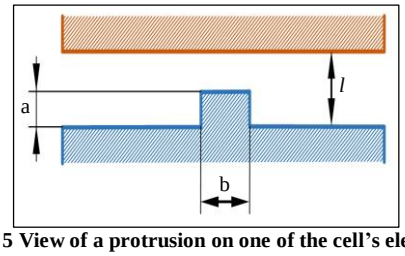

Fig. 5 View of a protrusion on one of the cell's electrodes

By conformally mapping the strip on the complex plane to the region on the complex plane corresponding to the gap between two electrodes with a protrusion on one of them [22], taking into account, we obtain the complex potential:

$$w = u + iv = -\frac{V}{2l}\left[2x + \frac{a\,sh\,\pi x}{\cos\pi y - ch\,\pi x}\right] + \\ +iV\left[1 - \frac{y}{l} + \frac{a\sin\pi y}{2l(\cos\pi y - ch\,\pi x)}\right]. \quad (26)$$

Using expression (16), we get:

$$E_x = -\frac{a\pi V \sin\pi y\, sh\,\pi x}{l^2(\cos\pi y - ch\,\pi x)^2}; \quad (27)$$

$$E_y = \frac{V\left[2 - \frac{a}{l}\pi + \cos 2\pi y + \left(\pi\frac{a}{l} - 4\right)\cos\pi y\, ch\,\pi x + ch\,2\pi x\right]}{2l(\cos\pi y - ch\,\pi x)^2}, \quad (28)$$

Where: $|\vec{E}| = \sqrt{E_x^2 + E_y^2}$.

Based on the obtained expressions, calculations were made of the distribution of the electric field strength over the surface with a protrusion in the case of a potential of 20 kV applied to the electrodes (Figures 6 and 7).

The results of the calculations showed that in the case of connecting a high-voltage voltage source in the center above the protrusion of the cell electrode (Figure 7), the difference in the distribution of the electric field intensity depending on the distance between the electrodes consists only in the amplitudes of the intensity, but the geometry does not change.

Accordingly, the value of the applied potential is determined by the sensitivity of the device's recording GDV of the bioobject, as well as the possibility of electrical breakdown. In addition, a decrease in the distance, as well as above, will lead to an increase in the maximum tension without its displacement relative to the middle of the studied biological object.

The situation looks different in the case of a shift of the voltage connection point from the middle of the protrusion by 10 mm (Figure 7). In this case, when the distance between the electrodes is mm (the distance from the protrusion to the second electrode of the cell is 1 mm), the distribution of the electric field intensity practically does not differ from the case when there is no shift.

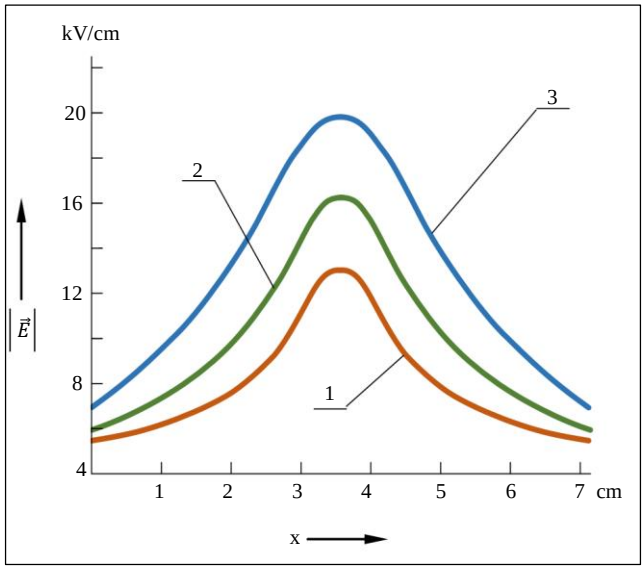

Fig. 6 Distribution of the electric field intensity over the protrusion of the cell electrode when *a* = *b* = 6 mm; *V* = 20 kV. Connecting the high-voltage voltage source in the center above the protrusion, i.e. without offset: 1) *l* = 7 mm; 2) *l* = 8 mm; 3) *l* = 10 mm.

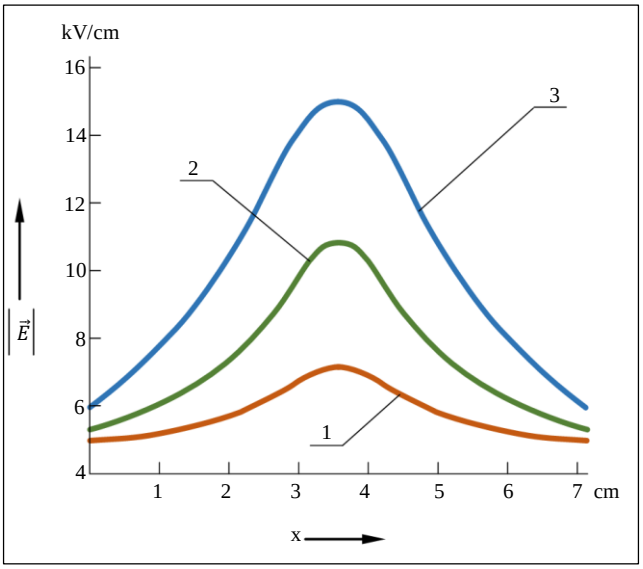

Fig. 7 Distribution of the voltage of the electric field over the protrusion on the electrode of the target, then *a* = *b* = 6 mm, *V* = 15 kV. Connecting the high-voltage voltage source in the center above the protrusion, i.e. without offset: 1) *l* = 7 mm; 2) *l* = 8 mm; 3) *l* = 10 mm

However, at distances (l = 8 mm, l = 10 mm), asymmetry in the field distribution begins to appear. Its maximum shifts towards the connection point, and its decline is steeper than its growth.

Thus, the displacement of the connection point away from the center of the protrusion does not allow obtaining a uniform GDV-gram of the entire biological object under study. It can be used only if it is necessary to study the border areas of the biological object.

In Figure 8, the graph of the modulus of the electric field above the protrusion when a = b = 6 mm, V = 15 kV is presented. The high-voltage voltage source is connected in

As follows from the given dependencies (Figure 7), a decrease in the voltage of the high-voltage source leads to a decrease in the stress modulus. If the distance between the protrusion and the second electrode of the device's GDV cell is more than 1.5 mm, the quality of GDV-grams will decrease. It may even lead to a complete cessation of the glow of the biological object.

To select the optimal pulse rate of high voltage pulses and assess the level of non-invasiveness of the method, it is necessary to estimate the energy of thermal processes and their impact on the biological object. The energy transferred by the discharge of the surface of the bio-object under study can be estimated by considering the processes in the discharge gas column. To do this, we calculate the power released in the discharge volume. The energy transferred in a single collision of an electron with an ion can be estimated by the expression [22, 23].

$$\Delta P = 2\frac{m_e}{m_i}\cdot\frac{m_e\cdot v_e}{2}, \quad (29)$$

Where m_e, m_i – the mass of the electron and the ion, respectively; v_e– electron speed. The transmitted power can be determined by the expression:

$$P = \int_0^\infty \frac{1}{\tau_e}\cdot\frac{2m}{m_i}\cdot\frac{m_e\cdot v_e^2}{2}\cdot dn(v_e), \quad (30)$$

Where $\tau_e = \frac{l}{v_e}$ – the inertia of time; l – mean free path length of an electron; $dn(v_e)$ – concentration of ion pairs of different signs (at time t).

Submitting dn as [22, 23]:

$$dn = f_o\cdot dv_e, \quad (31)$$

The expression for power will have the form:

$$P = \int_0^\infty \frac{1}{\tau_e}\cdot\frac{2m_e}{m_i}\cdot\frac{m_e\cdot v_e^2}{2}\cdot f_0 d\vec{v}_e, \quad (32)$$

Where $f_0 = C\cdot e^{-\frac{m_t\cdot v_t^2}{k\cdot T_e}}$ – Maxwell's function; k – became Boltzmann; T_e – electron temperature.

Given that the initial concentration of positive and negative ion pairs (at t = 0) equals n_0, value C in Maxwell's function is determined by the expression:

$$\int_0^\infty\int_0^\infty\int_0^\infty C\cdot e^{-a(v_x^2+v_y^2+v_z^2)}\cdot dv_x\cdot dv_y\cdot dv_z = n_0. \quad (33)$$

To calculate the integrals, we use the relation [11]:

$$2\int_0^\infty e^{-ax^2}dx = \left(\frac{\pi}{a}\right)^{1/2}.$$

Which leads to the expression:

$$\frac{C}{6}\cdot\left(\frac{\pi}{a}\right)^{\frac{3}{2}} = n_0, \quad (34)$$

Where $a = \frac{m_e}{2kT_e}$.

From expression (34), we obtain that:

$$C = 6\cdot n_0\left(\frac{a}{\pi}\right)^{\frac{3}{2}}. \quad (35)$$

To estimate the power, we consider that the electric field is applied along the "x" coordinate, and, accordingly, all ionization goes in this direction. In this case, the expression for power will have the form:

$$P = \int_0^\infty\int_0^\infty\int_0^\infty n_0\cdot\frac{\nu_{ex}}{l}\frac{m_e^2}{m_i}v_{ex}^2(\pi)^{-\frac{3}{2}}\times \\ \times e^{-\frac{m_e}{2kT_e}(v_x^2+v_y^2+v_z^2)}dv_x dv_y dv_z. \quad (36)$$

Solving equation (36) leads to the relation for power:

$$P = 6n_0\frac{1}{lm_i}\left(\frac{2m_e k^3 T_e^3}{\pi}\right)^{\frac{1}{2}}. \quad (37)$$

For the calculation, the following values of quantities typical for a low-current discharge were taken:

$n_0 = 10^{10}$ 1/m^3; $m_i = 10^{-26}$ kg; $\delta = 10^{-20}$ m^2; $E = 10^6$ V/m; $m_e = 10^{-30}$ kg; $n_i = 10^{25}$ 1/m^3; $kT = m_e{v_e}^2$; $l = \frac{1}{n_i\delta} = 10^{-6}$ m.

The speed of the electron is determined from the expression:

$$v_e = \sqrt{\frac{2eE}{m_e n_i \delta}} \approx \sqrt{\frac{3{,}2\cdot 10^{-19}\cdot 10^6}{10^{-30}\cdot 10^{26}\cdot 10^{-20}}} \approx$$

$$\approx \sqrt{3{,}2\cdot 10^{11}} \approx 0{,}56\cdot 10^6 \text{ m/s}.$$

$$kT = m_e\cdot {v_e}^2 = 10^{-30}\cdot 3{,}2\cdot 10^{11} =$$

$$= 3{,}2\cdot 10^{-19} \text{ kg·m}^2/\text{s}^2.$$

$$P = 6\cdot 10^{10}\cdot 10^6\cdot 10^{25}\sqrt{\left(\frac{2\cdot 10^{-30}\cdot(3{,}2\cdot 10^{-19})^3}{\pi}\right)} =$$

$$= 84\cdot 10^{-9} \text{ W/cm}^3 \text{ or } 0.084 \text{ μW/cm}^3.$$

As can be seen from the obtained results, even with the maximum values of the used parameters, the power released in the discharge is insignificant.

4. Results

According to the obtained expressions (19 – 25), calculations of the electric field between the electrodes of the cell were performed when the potential between them is equal to 15 and 20 kV (Figures 3 and 4). It follows from the graph (Figure 3) that the maximum intensity of the electric field is located above the middle of the recess and is 7 kV/cm at a voltage source of 15 kV. It follows from the graphs (Figure 4) that as the distance between the electrodes of the cell increases, the intensity of the electric field between them decreases, and the maximum intensity shifts to the point of connection of the voltage source.

According to the obtained expressions (27, 28), calculations were made of the distribution of the electric field strength over the surface with a protrusion in the case of a potential of 20 kV applied to the electrodes. The results of the calculations showed that in the case of connecting a high-voltage voltage source in the center above the protrusion of the cell electrode (Figure 6), the difference in the distribution of the electric field intensity depending on the distance between the electrodes is only in the amplitudes of the intensity, but the geometry does not change.

As follows from the given dependencies (Figure 7), a decrease in the voltage on the electrodes leads to a decrease in the stress modulus. If the distance between the protrusion and the second electrode of the device's GDV cell is more than 1.5 mm, the quality of GDV-grams will decrease and may even lead to a complete cessation of the glow of the bioobject. The energy transferred in one collision of an electron with an ion can be estimated by expression (29).

5. Discussion

From the performed calculations, it can be concluded that finding the optimal value of the applied potential is possible after experimental refinement of the obtained theoretical results. A complete and high-quality GDV image of a biological object can be obtained if a protrusion on one of the electrodes is used.

Using the concept of complex potential explained above, the distribution of the field between two flat electrodes of the cell of the GDV device was studied, taking into account the presence of a bioobject in the recess of the flat electrode and on the rectangular protrusion of one flat electrode.

Thus, based on the analysis of the electric field intensity distribution, it is possible to conclude that it is more effective

to place the electrode with the bioobject at a distance equal to 1 mm from the protrusion to the other electrode of the cell of the GDV device and to connect the high-voltage voltage source in the center of the protrusion without shifting. At smaller values of V –, the field strengths decrease, which will result in a lower quality of GDV-grams. As shown by the experimental research of the process of GDV of bio-objects, heat can be released in them during visualization with certain parameters of high-voltage pulses.

6. Conclusion

1. To describe the changes in the distribution of the electric field strength over the surface with protrusions on the electrode of the cell of the GDV device, on which the bioobject studied with the help of GDV is located, it is convenient to use the method of complex potentials, based on conformal mappings of a simple area on one complex plane to a real area, which is obtained on another complex plane.
2. In order to obtain a high-quality GDV-gram, the investigated bioobject should be placed on the surface of the protrusion of the cell electrode with a distance between the protrusion and the second electrode of the GDV device cell - 1 mm, and a high-voltage voltage source of 15...20 kV should be connected in the center of the protrusion without shifting.
3. In order to exclude the thermal impact of GDV on a biological object, the study of biological objects should be carried out at a power released in a discharge of no more than 0.08 μW/cm^3.

References

[1] Alfredo Flores, Jan Suszkiw, and Marcia Wood, "Radio Frequency Puts the Heat on Plant Pests," *Agricultural Research*, vol. 51, no. 2, pp. 15-17. 2003. [Google Scholar]

[2] Alfredo Flores, "Radio Frequencies Used to Kill Agriculture Pests," *Agricultural Research Service*, 2003. [Google Scholar]

[3] D.J.G. Eveke, and C. Brunkhorst, "Inactivation of in Apple Juice by Radio Frequency Electric Fields," *Journal of Food Science*, vol. 69, no. 3, pp. 134-138, 2006. [CrossRef] [Google Scholar] [Publisher link]

[4] M.M. Mofidian, H. Aliakbarian, and M.A. Mofidian, "Stored-Product Insects Protection Using Microwave Exposure," *Applied Electromagnetics Conference*, pp. 1-3, 2007. [Google Scholar]

[5] S.O. Nelson, "Electromagnetic and Sonic Energy for Insect Control," *Transactions of the ASAE*, vol. 9, no. 3, pp. 398-403, 1966. [CrossRef] [Google Scholar] [Publisher link]

[6] Stuart Nelson, "Dielectric Spectroscopy Applications in Agriculture," *3rd International Conference on Broadband Dielectric Spectroscopy and Its Applications*, Delft, Netherlands, 2004. [Google Scholar]

[7] S.O. Nelson, and L.E. Stetson, "Possibilities for Controlling Insects with Microwaves and Lower Frequency RF Energy," *IEEE Transactions on Microwave Theory and Techniques*, vol. 22, no. 12, pp. 1303-1305, 1974. [CrossRef] [Google Scholar] [Publisher link]

[8] S.O. Nelson, "Review and Assessment of Radio-Frequency and Microwave Energy for Stored-Grain Insect Control," *Transactions of the ASAE*, vol. 39, no. 4, pp. 1475-1484, 1996. [CrossRef] [Google Scholar] [Publisher link]

[9] O.I. Shapovalenko, T.I. Yanyuk, and A.F. Yanenko, "The Influence of Microwave Radiation on the Quality of Wheat Germs," *2000 10th International Crimean Microwave Conference. "Microwave and Telecommunication Technology"*, Crimea, Ukraine, pp. 576-577, 2000. [CrossRef] [Google Scholar] [Publisher link]

[10] J. Tang et al., "Postharvest Control of Insect Pests in Nuts and Fruits Based on Radio Frequency Energy," *ISHS Acta Horticultura*, vol. 599, pp. 175-181. 2003. [CrossRef] [Google Scholar] [Publisher link]

[11] "Insect Control in Nuts: A Review," *Agricultural Engineering*, vol. 10, no. 3&4, pp. 105-120, 2001.

[12] S. Wang et al., "Dielectric Properties of Fruits and Insect Pests as related to Radio Frequency and Microwave Treatments," *Biosystems Engineering*, vol. 85, no. 2, pp. 201-212, 2003. [CrossRef] [Google Scholar] [Publisher link]

[13] S. Wang et al., "Process Protocols Based on Radio Frequency Energy to Control Field and Storage Pests in In-Shell Walnuts," *Postharvest Biology and Technology*, vol. 26, no. 3, pp. 265-273, 2002. [CrossRef] [Google Scholar] [Publisher link]

[14] S. Wang et al., "Considerations in Design of Commercial Radio Frequency Treatments for Postharvest Pest Control in Inshell Walnuts," *Journal of Food Engineering*, vol. 77, no. 2, pp. 304-312, 2006. [CrossRef] [Google Scholar] [Publisher link]

[15] Steven L. Halverson, Timothy S. Bigelow, and Kathleen Lieber, "Penetration of Infested Stored-Products by EHF/SHF Microwave Energy," *Annual International Research Conference on Methyl Bromide Alternatives and Emissions Reductions*, 1998. [Google Scholar]

[16] Hadi Aliakbarian et al., "Agricultural Applications for Electromagnetic Exposure," *2007 Asia-Pacific Microwave Conference*, Bangkok, Thailand, pp. 1-4, 2007. [CrossRef] [Google Scholar] [Publisher link]

[17] James C. Lin, "Mechanisms of Electromagnetic Field Coupling into Biological Systems at ELF and RF Frequencies," *Advances in Electromagnetic Fields in Living Systems*, pp. 1-38, 2000. [CrossRef] [Google Scholar] [Publisher link]

[18] James C. Lin, "Microwave Property of Biological Materials," *Auditory Effects of Microwave Radiation*, pp. 73-96, 2021. [CrossRef] [Google Scholar] [Publisher link]

[19] Frank S. Barnes, and Ben Greenebaum, *Handbook of Biological Effects of Electromagnetic Fields - Two Volume Set*, 3rd ed., CRC Press, pp. 1-960, 2006. [CrossRef] [Google Scholar] [Publisher link]

[20] Gulzar Ahmad, *Electromagnetic Field Theory*, 1st ed., UET Peshawar, pp. 1-229, 2020. [Publisher link]

[21] Markus Zahn, *Electromagnetic Field Theory: A Problem-Solving Approach*, FL: Krieger Publishing Company, 1979. [Google Scholar] [Publisher link]

[22] George B. Arfken, Hans J. Weber, and Frank E. Harris, *Mathematical Methods for Physicists- A Comprehensive Guide*, 7th ed., Elsevier Academic Press, Inc., 2012. [Google Scholar] [Publisher link]

[23] Walter Thirring, *Classical Mathematical Physics-Dynamical Systems and Field Theories*, Springer-Verlag, New York, 1997. [CrossRef] [Google Scholar] [Publisher link]